

# Numerical Study of the Permeability Change Induced by Hot Water Injection in Deep Subsurface Thermal Energy Storage

Yonghui Huang<sup>1,2</sup>, Zhonghe Pang<sup>1</sup> and Georg Kosakowski<sup>3</sup>

<sup>1</sup>Key Laboratory of Shale Gas and Geoengineering, Institute of Geology and Geophysics, Chinese Academy of Sciences

<sup>2</sup>Department of Environmental Informatics, Helmholtz Centre for Environmental Research – UFZ

<sup>3</sup> Laboratory for Waste Management, Paul Scherrer Institute

[yh.huang@mail.iggcas.ac.cn](mailto:yh.huang@mail.iggcas.ac.cn)

**Keywords:** Two-phase flow; Reactive transport; Fine transport; Deep subsurface thermal energy storage.

## ABSTRACT

Seasonal storage of excess energy in deep subsurface is an essential technology for the efficient use and management of energy resources. Recently, deep subsurface thermal energy storage is rising in importance and attracting the attention of the researchers. Permeability plays a key role for successful thermal storage, particularly in the vicinity of the wells. During the process of subsurface thermal energy storage, the fluid-rock chemical equilibrium of a geothermal reservoir may become disturbed by the injection of hot water. Consequently, dissolution and precipitation reactions as well as the fine transport might result in permeability damage. Understanding the permeability and porosity alteration is critical in predicting fluid migration in the subsurface and long-term operation efficiency of the thermal storage system. Here, we present a novel continuum non-isothermal reactive transport model that captures and predicts the spatial pattern of permeability and porosity evolution in a sandstone reservoir. The model considers mineral dissolution and precipitation under the influence of the temperature change, and tracks the potential feedbacks between flow, heat transfer, chemical reactions and fines transport. The developed model is validated by replicating the existing core flooding experimental measurements (Rosenbrand et al., 2014) of the porosity reduction and the evolving silica and calcite concentration. Subsequently, by simulating the thermal storage in the deep subsurface at the field scale, the long-term evolution of the rock permeability is predicted.

## 1. INTRODUCTION

Seasonal storage of excess energy in deep subsurface is an essential technology for the efficient usage and management of the energy resources. In China, there typically exists temporal and spatial mismatch between the supply and the demand for heat. Subsurface energy storage is an efficient solution to bridge the gaps. Shallow and low to intermediate temperature aquifer thermal storage has undergone significant developments in the past century (Fleuchaus et al. (2018)). Recently, the high temperature (70-150°C) thermal storage in deep subsurface receives more attention due to its significant advantages and values (Drijver, (2017)).

The injection of such high temperature water inevitably disturbs the thermodynamic equilibrium and modifies the porous medium microstructure, which can lead to chemical reactions and fines migration. Temperature is known to exert an important control on both reactions of minerals and fines transport in the aquifer. Generally, elevated temperature increases dissolution/precipitation rates in the aquifer which may affect the permeability of the aquifer (Holmslykke et al. (2017)). On the other hand, high temperature has a strong influence on the transport of suspensions and colloids in porous media with particle capture, which further decreases permeability by detachment and mobilization of fine particles and their migration/straining in narrow pore throats (You et al. (2015), Civan (2010)). Therefore, the permeability change due to the injection of hot water is one of the main concerns in deep subsurface aquifer thermal energy storage, and keeps attracting the attention of both researchers and engineers.

Sbai and Azaroual (2011) presented a numerical model to predict permeability damage due to fines migration during CO<sub>2</sub> sequestration, but their model did not consider thermal effect. You et al. (2015) presented the first quantitative analysis of temperature effects on the forces exerted on particles and of the resultant migration of fines. Rosenbrand et al. (2015) conducted core experiments to investigate the effects of temperature on permeability reduction by fines migration and they found that heating the core sample from 20 to 80 °C reduced the permeability, and the main course is the mobilization of the fine particle. Othman et al (2019) conducted experiments and found fine migration and its consequent mineral dissolution/precipitation determine the core samples' permeability, so they proposed the necessity of taking both fine transport and chemical reaction into account. Despite significant progress in both areas, the permeability evolution induced by both fine transport and chemical reactions under non-isothermal conditions remains an unsolved problem.

In this work, a novel numerical model is set up that couples the two-phase flow, heat transfer, particle transport and chemical reactions. The model aims to investigate the permeability change during the hot water injection for deep subsurface thermal energy storage, which is caused by the interaction between particle transport and chemical reaction. A five-spot numerical example (proposed in Sbai and Azaroual, 2011) is selected to evaluate the model and demonstrate the potential application at a site scale.

## 2. MATHEMATICAL FRAMEWORK

In this work, due to the high temperature and high pressure in the context of the deep subsurface thermal energy storage, a two-phase condition is assumed for the geothermal formation (i.e. water phase and vapor phase). The mathematical framework is based on the two-phase flow transport to predict spatial distribution of the pressure, phase velocities, and the water saturation. Then it is complemented by a solute transport equation in the aqueous phase for calculating the chemical component distribution and transport which might be triggered by the mineral dissolution and precipitation. Particle transport processes are described through a set of coupled convection – diffusion equations for each subset of fine particles. The thermal effects are depicted by the energy conservation equations.

Quantitative assessment of the permeability variation is strongly dependent on the accuracy of experimental data on permeability – porosity relationships, in which the thermal effects are included.

### 2.1 Two-phase Flow of Vapor and Water Phases

Two-phase fluid flow equations are formulated based on the mass conservation for each phase. We consider here the non-isothermal two-phase fluid flow transport equations with respect to the global pressure,  $p$ , and liquid saturation,  $S_w$  of two immiscible fluids.

$$\phi c_t \frac{\partial p}{\partial t} = \nabla \cdot [\mathbf{K} \lambda_t (\nabla p - (f_l \rho_l + f_g \rho_g) g \nabla z)] + \frac{q_l}{\rho_l} + \frac{q_g}{\rho_g} \quad (1)$$

Where  $\phi$  is the porosity,  $\mathbf{K}$  is the intrinsic permeability,  $\rho_w$  and  $\rho_g$  are the density of the liquid phase and gas phase, respectively,  $\lambda_t$  is the total mobility, and it is defined as  $\lambda_t = \lambda_l + \lambda_g$ , while  $\lambda_l = \frac{k_{rel,l}}{\mu_l}$  is the mobility of the liquid phase, and  $k_{rel,l}$  is the relative permeability of liquid phase, and  $\mu_l$  is the viscosity of the liquid phase.  $f_w$  and  $f_g$  are the fractional flow function of liquid and gas phase:  $f_w = \lambda_w / \lambda_t$ ,  $q_w$  is a time-dependent source/sink term of liquid phase;

$$\phi \frac{\partial S_l}{\partial t} = -\nabla \cdot [f_c \mathbf{u} - \mathbf{K} f_c \lambda_l \Delta \rho g \nabla z] + \frac{q_g}{\rho_g} \quad (2)$$

Where  $\mathbf{u} = \mathbf{u}_l + \mathbf{u}_g$  the total fluid flow velocity,  $\Delta \rho = \rho_l - \rho_g$  is the density difference between liquid phase and gas phase,

The total fluid flow velocity  $\mathbf{u}$  dependence on the pressure is described by generalized Darcy law and given as follows:

$$\mathbf{u} = -\mathbf{K} \lambda_t (\nabla p - (\rho_l f_l + \rho_g f_g) g \nabla z) \quad (3)$$

Here for simplicity, we ignore the capillary pressure, and assume the gas pressure equals to the liquid phase pressure. We enclose the system with further closure equations

### 2.2 The Energy Balance Equation

Energy conservation equation is applied here to account for the conduction of heat in the rock and advection of enthalpy by fluid, which is given by:

$$\frac{\partial H_t}{\partial t} = -\nabla \cdot (\rho_l h_l \mathbf{v}_l) - \nabla \cdot (\rho_g h_g \mathbf{v}_g) + \nabla \cdot (K_T \nabla T) + Q_{\text{heat}} \quad (4)$$

Where  $h_l$  and  $h_g$  are the enthalpy of the liquid and gas phase,  $\mathbf{v}_l$  and  $\mathbf{v}_g$  are the Darcy velocity of the liquid and gas phase.  $K_T$  is the thermal conductivity,  $H_t$  represents the total enthalpy, which contains the contributions both from the fluid (gas and water) and the rock, and its time derivative is defined as:

$$\frac{\partial H_t}{\partial t} = \frac{\partial(\phi H_f)}{\partial t} + (1 - \phi) \rho_r c_{pr} \frac{\partial T}{\partial t} \quad (5)$$

Where  $H_f$  is the enthalpy of the fluid:  $H_f = S_l \rho_l h_l + S_g \rho_g h_g$ ,  $\rho_r$  is density of the rock,  $c_{pr}$  is the specific heat capacity of the rock.

### 2.3 The Component Transport Equation

In this section, equations describing the solute transport and chemical reactions are presented. The governing equations describing the advection-diffusion transport of solutes are structured in terms of independent component concentrations:

$$\frac{\partial(\phi c_f^i)}{\partial t} = -\nabla \cdot (\rho_l c_l^i \mathbf{v}_l) - \nabla \cdot (\rho_g c_g^i \mathbf{v}_g) + V + Q_i + q_i \quad (6)$$

Where  $C_f^i$  is the total volumetric concentration of the  $i$ -th component, and it is defined as:  $C_f^i = S_l \rho_l c_l^i + S_g \rho_g c_g^i$ .  $Q_i$  represents the source /sink term, while  $q_i$  represents the chemical reaction rate that accounts for the mineral dissolution and precipitation:  $q_i = \partial((1 - \phi) \rho_r c_{ri}) / \partial t$

This is further solved by a chemical reaction solver (Yapparova et al. (2019)).

## 2.4 The Particle Transport

The mass balance equation for suspended, attached and strained fines in porous media is:

$$\frac{\partial(\phi c + \sigma_s + \sigma_a)}{\partial t} + \alpha U \frac{\partial c}{\partial x} = 0 \quad (7)$$

Where  $\sigma_s$  are  $\sigma_a$  are the concentrations of attached and strained fines, factor  $\alpha$  accounts for slow particle motion. Particle straining rate is proportional to the suspended particle transport flux,

$$\frac{\partial \sigma_s}{\partial t} = \lambda \alpha U c \quad (8)$$

Consider flow with fines mobilization, where the attached fine particle concentration is given by the maximum retention function  $\sigma_{cr}$  as follows:

$$\sigma_a = \sigma_{cr}(|U|) \quad (9)$$

Darcy's law accounts for permeability damage due to straining can be formulated as:

$$U = -\frac{k(\sigma_s)}{\mu} \frac{\partial p}{\partial x}, \quad k(\sigma_s) = \frac{k_0}{1 + \beta \sigma_s} \quad (20)$$

$\beta$  is the formation damage coefficient,  $k_0$  is the formation permeability. The particle transport mathematical work is described in detail in You et al (2016).

## 2.5 Numerical Solution

For the coupled system, the standard Galerkin finite element method is employed for spatial discretization, with a fully implicit backward Euler scheme for the time integration. Application of these space and time discretization schemes to the governing equations leads to a coupled system of discrete residual equations with high nonlinearity. The Newton method with line search scheme is employed for the linearization, while a GMRES solution strategy with ILUT preconditioning is applied to solve the linear equation system. The coupling between flow transport and chemical reaction can be found in (Huang et al (2018), Kosakowski and Watanabe (2014)). All the simulation work is carried out based on the platform of OpenGeoSys V6. (Kolditz et al. (2012)).

## 3. NUMERICAL SIMULATION

In this section, numerical experiment benchmarks are discussed to validate the numerical model and further investigate the permeability evolution during the hot water injection.

### 3.1 Hot water injection into heterogeneous geothermal reservoir

In this example, we simulate the hot water injection and production in a heterogeneous geothermal reservoir, which resembles to the process of the deep subsurface thermal energy storage. This example is based on the benchmark proposed in Sbair and Azaroual (2011). A 2-D permeability distribution are extracted from the full three-dimensional permeability field used by the SPE-10 comparative solution project (Christie and Blunt (2001)), and it is characterized as a high-contrast heterogeneous porous medium. While the porosity is strongly correlated with the horizontal permeability. The porosity and permeability distribution are presented in Figure 1.

The selected layers hold a scale of 365.76 m  $\times$  670.56 m  $\times$  0.6096 m. The reservoir parameters, initial values, production data, and other extra parameters for particle release, transport, and capture are given in Table 1. The production well is located at the four corners of the domain, and the injection well is in the center. Here, the water phase is extracted from four production wells at the domain corners with an equal flow rate and water is injected into the formation from an injection well in the center. The injected water temperature is higher than the original formation water temperature.

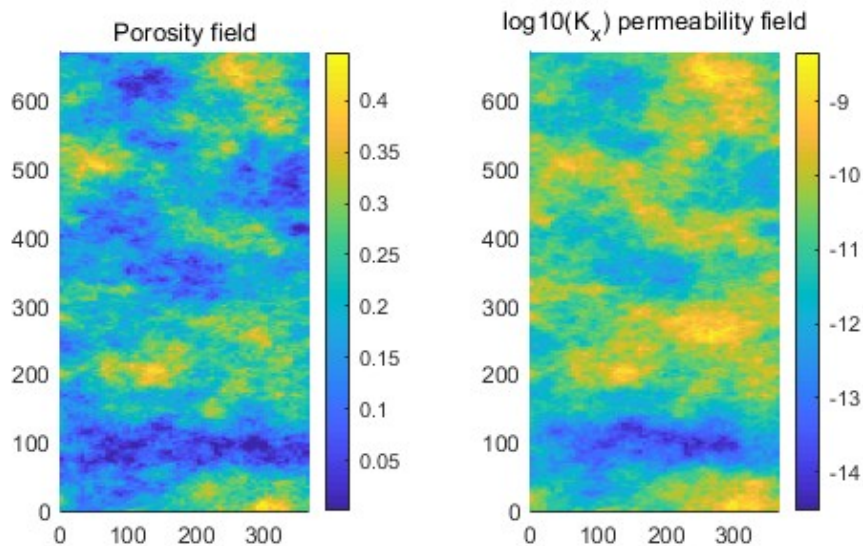
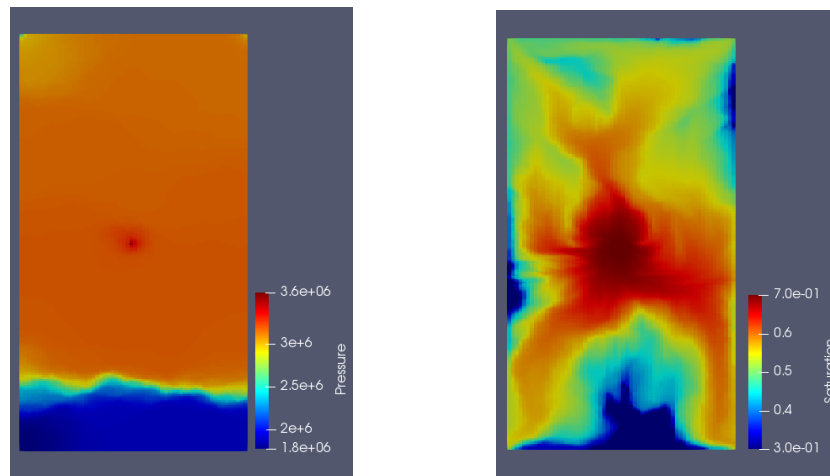
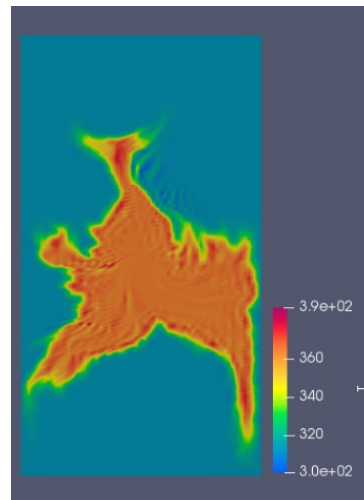


Figure 1: Porosity and permeability distribution field for the simulation

**Table 1: Parameters used for studying hot water injection into two-dimensional heterogeneous layers extracted from SPE-10 comparative solution project.**

Parameters of the geological model	Value	Unit
Reservoir scale	365.76×670.56×0.6096	m
Number of FE cells	13200	-
Initial pressure	30	MPa
Viscosity of vapor	1e-3	kg/(m s)
Viscosity of water	1e-5	kg/(m s)
Residual saturation of water	0.3	-
Residual saturation of vapor	0.3	-
Initial temperature	313	K
Injection rate	25	m <sup>3</sup> /h
Injection Temperature	363	K
Production rate	6.25	m <sup>3</sup> /h

Figure 2 gives the pressure and saturation distribution after one-month of hot water injection. It can be observed the maximum pressure and saturation are located in the vicinity of the injection well. Figure 3 presents the temperature distribution. The attached and strained particle concentrations are shown in Figure 4.

**Figure 2: Simulation results for hot water injection after 1 month in terms of pressure and saturation****Figure 3: Simulation results for hot water injection after 1 month in terms of temperature distribution**

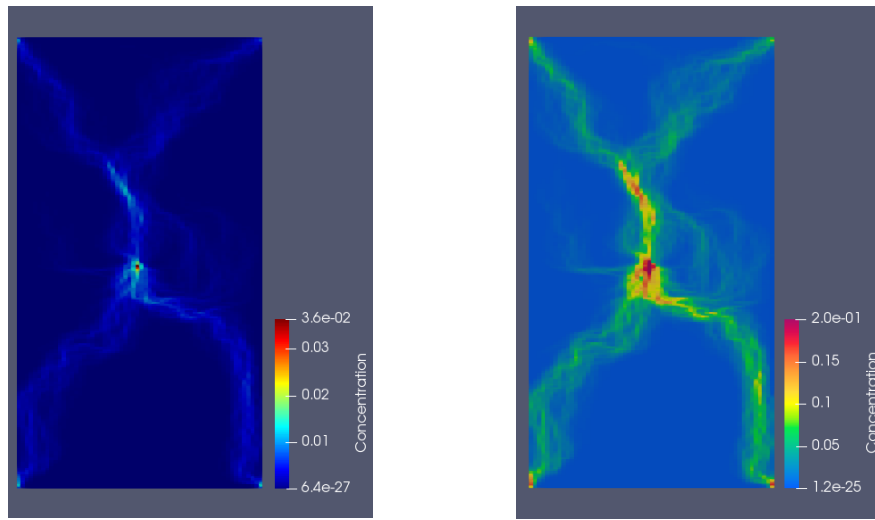


Figure 4: Simulation results for hot water injection after 1 month in terms of attached and strained fines concentration

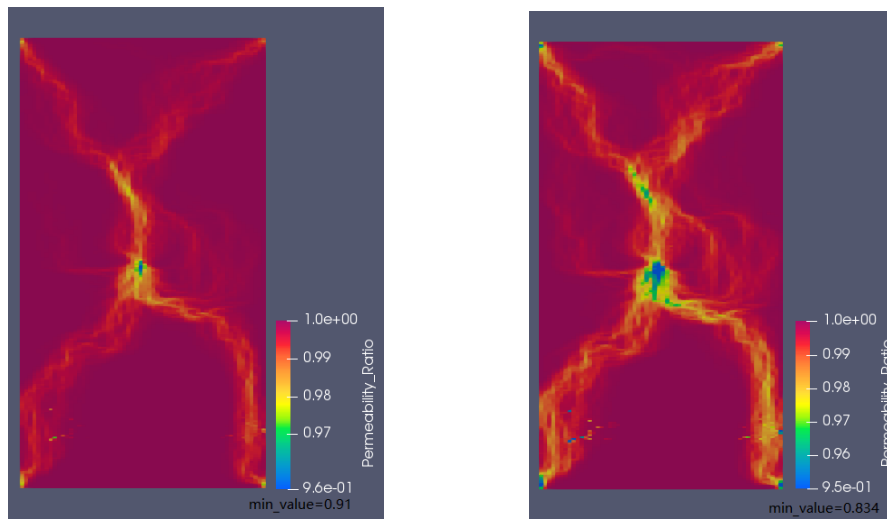


Figure 5: Simulation results for hot water injection (at different temperature: 363 K (left), 393 K (right)) after 1 month in terms of permeability decline ratio ( $K_{\text{current}}/K_{\text{previous}}$ )

From Figure 5 (left), a permeability decrease of around 10% is observed nearby the injection well. The permeability decrease distribution is similar to the concentration of the attached and strained fines as shown in Figure 4. While if we increase the injection temperature to 393 K, the minimum permeability decline ratio decreases to 0.834, and approximately a 15% permeability decrease near the injection well, which can be seen at Figure 5 (right). This indicates that higher temperature leads to more severe permeability decline at this condition. The permeability decline curve with respect to the injection time are plotted at the point 5 m in the Figure 6, and a linear permeability decline trend can be also found. Moreover, it is noted that severe permeability decline is also found near the vicinity of the production well.

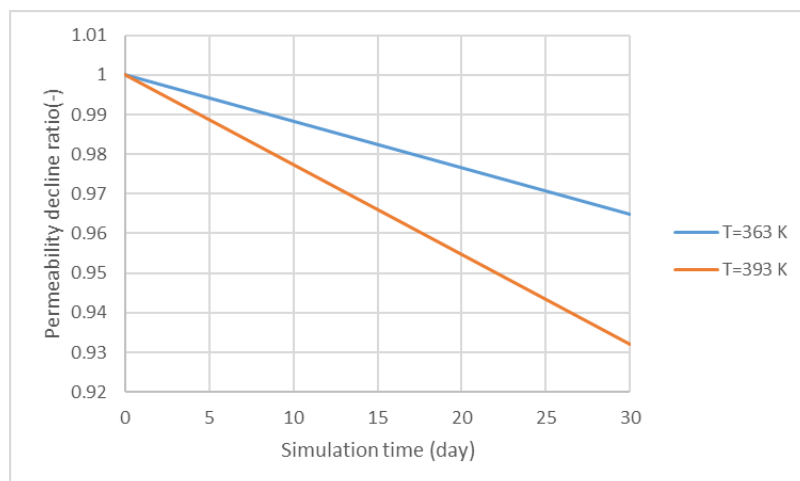


Figure 6: Permeability decline at the point 5 m from the injection well at different injection temperature.

#### 4. DISCUSSION

It can be observed from Figure 3 that the severe numerical oscillation is exhibited in the temperature distribution, which is more significantly demonstrated in Figure 7. This figure presents a cross-section profile curve of temperature. These numerical oscillations typically happen in the standard Galerkin discretization problem, especially in the advection dominated transport problems (Helmig and Huber, (1998)). These problems can be overcome by applying the Petrov-Galerkin method or Streamline-upwind Petrov-Galerkin method (SUPG), as well as the fully upwind method.

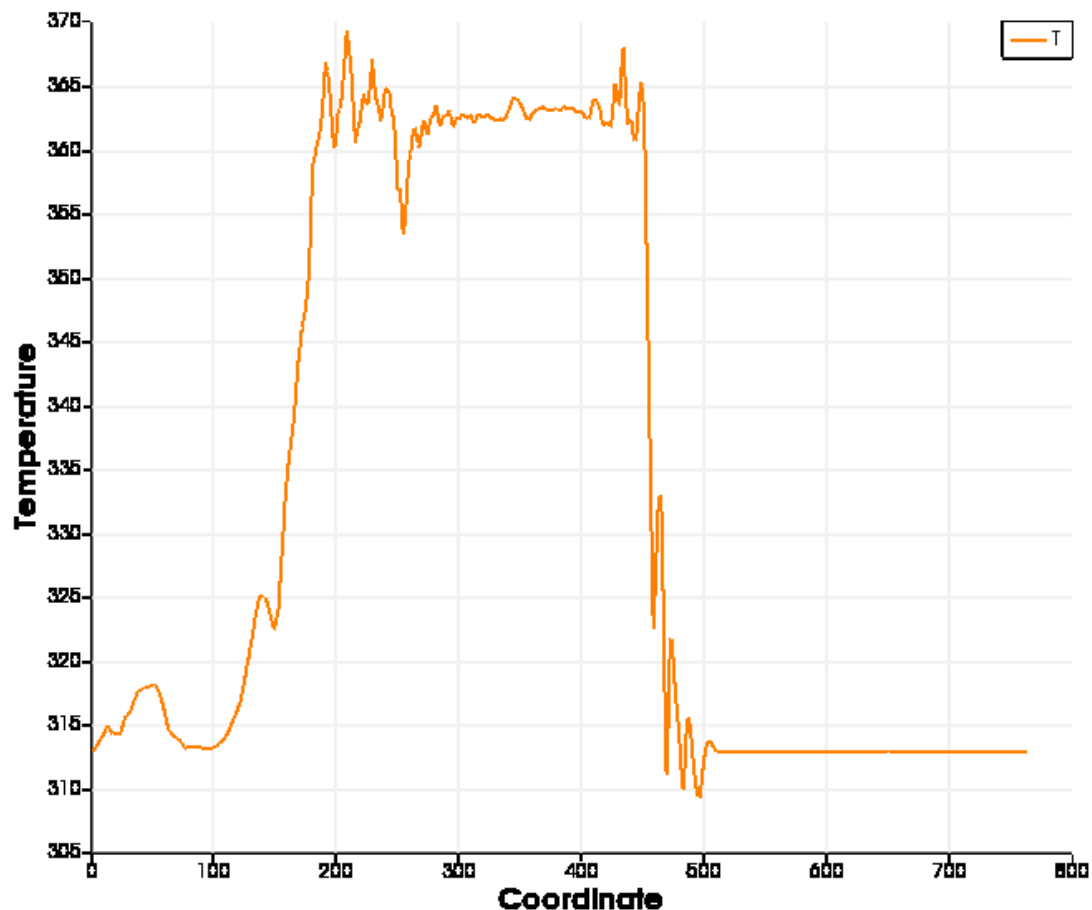


Figure 7: Numerical oscillation of temperature cross-section profile curve

#### 5. CONCLUSION AND OUTLOOK

This work presents a numerical study of the permeability evolution during the hot water injection in deep subsurface thermal storage system. The permeability variation in the geothermal formation can be caused by fine particle transport or mineral dissolution/precipitation induced by chemical reactions. Meanwhile, fine particle transport mechanism is highly coupled with the chemical reactions and they interact with each other.

Proper formulation of the fine migration and chemical reactions in two-phase flow transport condition in porous media considering the effect of temperature is presented, and an accurate numerical solution based on the finite element method was completed successfully. Hence, the model presented in this work provides a scientific insight into the permeability evolution induced by fine particle transport and chemical reactions.

The model is further applied to the benchmarks considering the hot water injection into a heterogeneous reservoir at site scale. This study demonstrates that hot water injection has a significant effect on permeability impairment. In the application considered above, the permeability decline is more severe under high-temperature and non-isothermal conditions. Increasing the injection temperature can enhance the permeability impairment.

Consequently, for future work, comprehensive experiments measuring all the relevant fluid and porous material properties, capturing the key mechanism of particle attachment and strain, as well as the chemical reactions taken place in the formation, shall be conducted to further validate the numerical model; especially for the parameters used for fine transport and chemical reactions.

#### ACKNOWLEDGEMENTS

This research is supported by the Strategic Priority Research Program of Chinese Academy of Sciences, Grant No. XDA 21050500.

## REFERENCES

- Rosenbrand, E., Haugwitz, C., Sally, P., Jacobsen, M., Kj  ller, C. and Lykke, I.: Geothermics The effect of hot water injection on sandstone permeability, *Geothermics*, **50**, (2014), 155–166.
- Othman, F., Naufaliansyah, M. A., and Hussain, F: Effect of water salinity on permeability alteration during CO<sub>2</sub> sequestration, *Advances in Water Resources*, **127**, (2019), 237-251.
- You, Z., Yang, Y., Badalyan, A., Bedrikovetsky, P., and Hand, M. Mathematical modelling of fines migration in geothermal reservoirs. *Geothermics*, **59**, (2016), 123-133.
- Civan, F. Non-isothermal permeability impairment by fines migration and deposition in porous media including dispersive transport. *Transport in porous media*, **85**(1), (2010), 233-258.
- Holmslykke, H. D., Kj  ller, C., & Fabricius, I. L. Core Flooding Experiments and Reactive Transport Modeling of Seasonal Heat Storage in the Hot Deep Gassum Sandstone Formation. *Acs Earth and Space Chemistry*, **1**(5), (2017), 251-260.
- Sbai, M. A., and Azaroual, M. Numerical modeling of formation damage by two-phase particulate transport processes during CO<sub>2</sub> injection in deep heterogeneous porous media. *Advances in Water Resources*, **34**(1), (2011), 62-82.
- Yapparova, A., Miron, G. D., Kulik, D. A., Kosakowski, G., and Driesner, T. An advanced reactive transport simulation scheme for hydrothermal systems modelling. *Geothermics*, **78**, (2019), 138-153.
- Christie MA and Blunt MJ. Tenth SPE comparative solution project: a comparison of upscaling techniques. *SPE Reserv Eng Eval*, **4**(4) (2001), 308 – 17.
- Helmig, R., and Huber, R. Comparison of Galerkin-type discretization techniques for two-phase flow in heterogeneous porous media. *Advances in Water Resources*, **21**(8), (1998), 697-711.
- Kolditz, O., Bauer, S., Bilke, L., B  ttcher, N., Delfs, J. O., Fischer, T., ... and Park, C. H. OpenGeoSys: an open-source initiative for numerical simulation of thermo-hydro-mechanical/chemical (THM/C) processes in porous media. *Environmental Earth Sciences*, **67**(2), (2012), 589-599.
- Kosakowski, G., and Watanabe, N. OpenGeoSys-Gem: a numerical tool for calculating geochemical and porosity changes in saturated and partially saturated media. *Physics and Chemistry of the Earth, Parts A/B/C*, **70**, (2014), 138-149.
- Huang, Y., Shao, H., Wieland, E., Kolditz, O., and Kosakowski, G. A new approach to coupled two-phase reactive transport simulation for long-term degradation of concrete. *Construction and Building Materials*, **190**, (2018), 805-829.
- Martinez, J. D.. Water-Mineral Reactions Related to Potential Fluid-Injection Problems: Discussion. (1972).
- Drijver B. High temperature aquifer thermal energy storage (HT-ATES) - water treatment in practice. Utrecht, The Netherlands: Nationaal Congres Bodemenergie; 2011
- Fleuchaus, P., Godschalk, B., Stober, I., and Blum, P. Worldwide application of aquifer thermal energy storage–A review. *Renewable and Sustainable Energy Reviews*, **94**, (2018), 861-876.
- You, Z., Bedrikovetsky, P., Badalyan, A., and Hand, M. Particle mobilization in porous media: temperature effects on competing electrostatic and drag forces. *Geophysical Research Letters*, **42**(8), (2015), 2852-2860.
- Othman, F., Naufaliansyah, M. A., and Hussain, F.. Effect of water salinity on permeability alteration during CO<sub>2</sub> sequestration. *Advances in Water Resources*, **127**, (2019), 237-251.